Lithos 358–359 (2020) 105418

Contents lists available at ScienceDirect

Lithos

journal homepage: www.elsevier.com/locate/lithos

Research Article

Timescales of magmatic processes in post-collisional potassic lavas, northwestern Tibet

Haibo Zou [a,b,*], Jorge Vazquez [c], Qicheng Fan [d]

[a] Department of Geosciences, Auburn University, Auburn, AL 36849, USA
[b] State Key Laboratory of Continental Dynamics, Department of Geology, Northwest University, Xi'an 710069, China
[c] U.S. Geological Survey, 345 Middlefield Road, Mail Stop 910, Menlo Park, CA 94025, USA
[d] Institute of Geology, China Earthquake Administration, Beijing 100029, China

ARTICLE INFO

Article history:
Received 6 October 2019
Received in revised form 5 February 2020
Accepted 6 February 2020
Available online 12 February 2020

Keywords:
^{238}U-^{230}Th disequilibrium
Dating young zircons
High-resolution timescales
Continental collision zones
Magma storage
Tibetan Plateau magmatism

ABSTRACT

Post-collisional potassic volcanic rocks on the Tibetan Plateau are widespread, but geologically young (<375 ka) volcanism suitable for ^{238}U-^{230}Th geochronology is rare on the plateau. The geologically young Ashikule volcanic field from northern Tibet offers an excellent opportunity for studying high-resolution timescales of magmatism in continental collision zones. Here we report U-Th crystallization ages of zircons from Ashishan volcano and Wulukeshan volcano within the Ashikule volcanic field. In this study, we have identified 3 pulses of zircon crystallization at circa 70 ka, 105 ka, and 290 ka for Ashishan volcanic rocks and 1 pulse of zircon crystallization at circa 115 ka for Wulukeshan. Comparison of high-resolution zircon crystallization ages of 70 ka and 105 ka with respective eruption ages indicate that the zircon crystal residence time for the Ashishan volcano is short (<5 kyr). The presence of 290-ka zircon in a different Ashishan lava flow suggests the 270-ka volcanic pulse previously reported for other volcanoes in Ashikule volcanic field also occurred at Ashishan. The zircon crystallization age of ~115 ka for Wulukeshan volcano suggests that Wulukeshan volcano erupted later than previously inferred. Similar zircon age spectrums of ~105–115 ka for Ashishan and Wulukeshan volcanoes suggest a common interconnected subsurface magma reservoir for these two young volcanoes during Pleistocene time. Our new high-resolution U-Th zircon age data reveal that post-collisional potassic magmas below northern Tibet erupted soon after their formation (<5 kyr), in spite of their passage through thick continental crust. The high abundance (~60%) of geologically old (>375 ka) zircons demands for crystal-scale isotope studies of the widespread post-collisional lavas in continental collision zones, as the complexities cannot be resolved by bulk analysis methods alone.

1. Introduction

Widespread post-collisional potassic volcanism has been occurring since about 45 million years ago on the Tibetan Plateau (e.g., Xia et al., 2011), the largest active continental collision zone on Earth (Fig. 1). The geochemical characteristics and timing of these post-collisional volcanoes have been used to constrain the chemical and thermal structure of the lithosphere in this unique tectonic setting, and the timing and deep processes inducing plateau uplift and growth (e.g., Chen et al., 2012; Chen et al., 2013; Cooper et al., 2002; Deng, 1978; Ding et al., 2003b; Flower et al., 1998; Liu et al., 2014; Miller et al., 1999; Turner et al., 1996; Wang et al., 2008). Extensive petrological and Nd-Sr-Pb isotopic studies of these potassic lavas (Chen et al., 2012; Chung et al., 2005; Ding et al., 2003a; Flower et al., 1998; Gao et al., 2007; Guo et al., 2006; Mo et al., 2007; Turner et al., 1996; Williams et al., 2004) have established the chemical heterogeneity of the mantle source beneath the Tibetan Plateau. By contrast, our understanding of the timescales and processes of magma evolution beneath thick continental collision zones is lagging behind. In order to resolve the usually short timescales of magmatic processes, young (<350 ka) volcanic rocks and ^{238}U-^{230}Th disequilibrium are required.

The Ashikule volcanic field (AVF) is unique in representing a rare occurrence of young eruptions of trachyandesites (4.0–4.4 wt% K_2O; Cooper et al., 2002) on the northern Tibetan Plateau. The trachyandesites from Ashikule are geochemically similar to those older Cenozoic examples from the northern Tibetan Plateau. Because of their young ages, dating of pre-eruptive crystallization can be achieved at high resolution, i.e. uncertainties of 10^3–10^4 years, using the ^{238}U-^{230}Th disequilibrium method.

* Corresponding author at: Department of Geosciences, Auburn University, Auburn, AL 36849, USA.
E-mail address: hzz0006@auburn.edu (H. Zou).

https://doi.org/10.1016/j.lithos.2020.105418

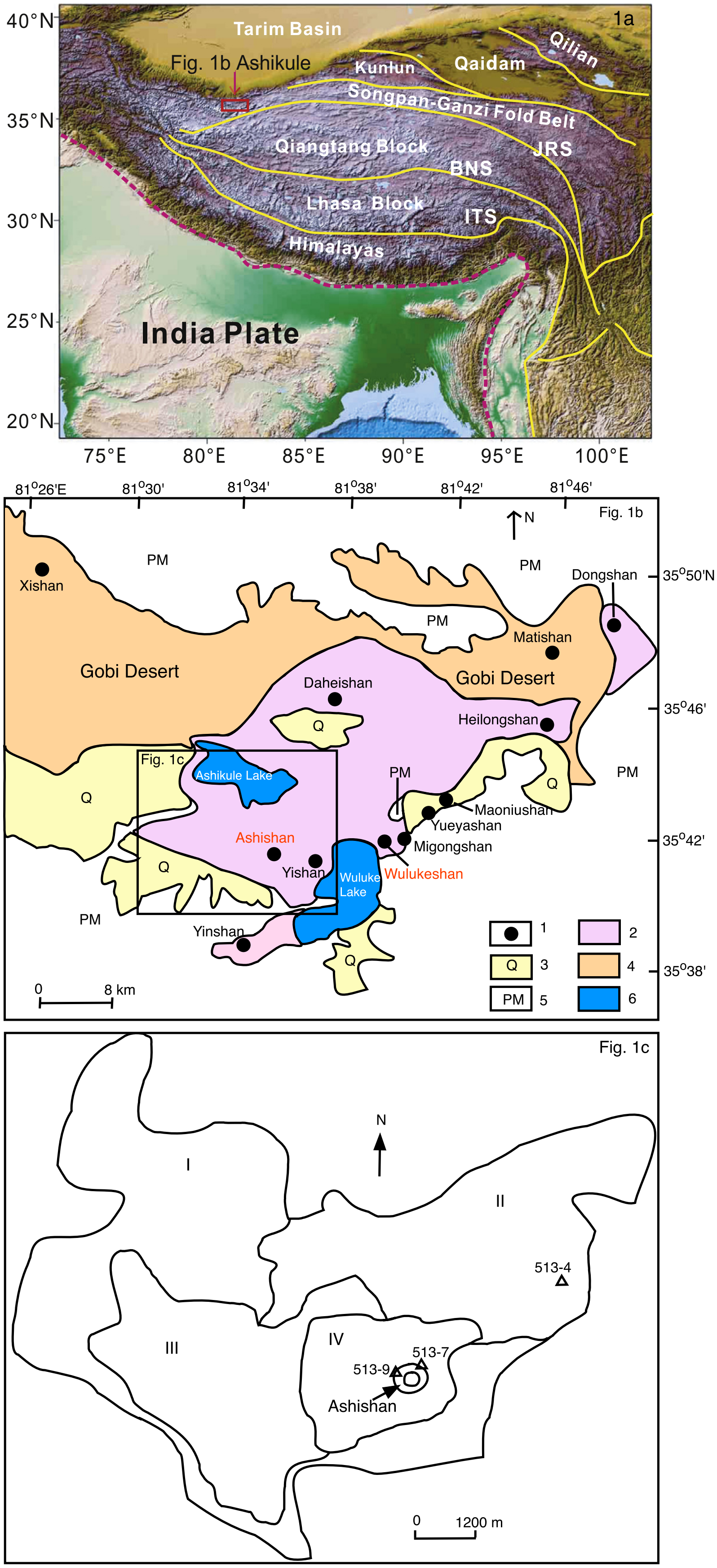

Fig. 1. (a) Simplified map of the Tibetan Plateau (Liu et al., 2017). Ashikule volcanic field (rectangle) is located in northern Tibet. ITS = Indus-Tsangpo suture; BNS = Bangong-Nujiang suture; JRS = Jinshan River suture. (b) Map of Ashikule volcanic field (Yu et al., 2014). Legends: 1, Volcanoes; 2, Holocene to Middle Pleistocene volcanic rocks; 3, Q = Holocene sediments; 4, Gobi Desert; 5, PM = pre-Mesozoic rocks (Yu et al., 2014); 6, Lakes. (c) Map of the Ashishan volcano (Shen et al., 2014) and sample locations. I-IV units represent different lava flows. The small circle is the Ashishan cone.

In this study, we have dated zircons from the two youngest volcanoes, Ashishan and Wulukeshan, from the AVF in order to resolve the timescales of magmatic evolution and pre-eruption storage for potassic magmas erupted in continental collision zones. The results of our study provide new insights into (1) the relations between the products of volcanism and their associated subvolcanic magmatic system; (2) the interconnectivity of the crustal magmatic system beneath Ashishan and Wulukeshan.

2. Geologic background

The post-collisional lavas on the Tibetan Plateau are distributed in both northern Tibet (45–26 Ma volcanic rocks in Qiangtang terrane, and 20 Ma to recent volcanic rocks at Songpan-Ganzi, Kunlun, and western Qiangtang terranes) and southern Tibet (26–8 Ma volcanic rocks in Lhasa terrane) (Xia et al., 2011). They are generally potassic to ultrapotassic, and are characterized by large enrichments in incompatible elements, and by unradiogenic Nd isotope ratios and radiogenic Sr and Pb isotope ratios. Compared with the highly heterogeneous 26–8 Ma volcanic rocks from southern Tibet (Lhasa block) ($^{87}Sr/^{86}Sr$ = 0.7107–0.7365, $\varepsilon_{Nd} = -8$ to -15), the post-collisional lavas in northern Tibet (Qiangtang, Songpan-Ganzi, Kunlun) show more restricted variations in Nd and Sr isotopic compositions ($^{87}Sr/^{86}Sr = 0.7071$–0.7105, $\varepsilon_{Nd} = -2$ to -8) and have a smaller proportion of ultra-potassic lavas (Zhao et al., 2009).

The Ashikule volcanic field (AVF) is located in the Ashikule basin, a Quaternary basin (750 km^2) in western Kunlun Mountain at the northwestern Tibetan Plateau, just south of Tarim Craton. The AVF comprises a dozen volcanic centers (Fig. 1b) and widespread lava flows that cover an area of 250 km^2 (1/3 of the Ashikule Basin). The total eruption volume is about 20 km^3 (Guo et al., 2006). The elevations of these volcanoes range from 4800 m to 5100 m, representing some of the highest Quaternary volcanoes on Earth. Due to the remoteness, high elevation, and the harsh and nearly inaccessible field conditions, the magmatic evolution leading to the volcanic rocks from AVF is poorly known.

The AVF volcanic rocks are potassic mafic to intermediate lavas, representing the more mafic samples from northern Tibetan Plateau. The dominant rock types at AVF are trachyandesite and basaltic trachyandesite. Their chemical composition and Nd—Sr isotopic compositions ($^{87}Sr/^{86}Sr = 0.7091$–0.7104, $\varepsilon_{Nd} = -5.0$ to -8.0) (Cooper et al., 2002; Guo et al., 2006; Turner et al., 1993) are similar to other lavas from northern Tibet Geochemical Province ($^{87}Sr/^{86}Sr$ = 0.7071–0.7105, $\varepsilon_{Nd} = -2$ to -8) (Zhao et al., 2009). The AVF lavas are porphyritic with 10–20% phenocrysts embedded in a glassy and fine-grained groundmass. The phenocrysts mainly consist of clinopyroxene and plagioclase, with minor olivine and alkali feldspar in some samples. Groundmass in most samples is glass, and some samples have microcrystalline plagioclase, alkali feldspar, pyroxene, and Fe-Ti oxides.

Volcanism at AVF started at 2.8 Ma at Xishan in the northwest part of the Ashikule Basin (Fig. 1b). The volcanoes in the AVF can be divided into 3 groups according to their eruption ages and the extent of preservation of volcanic cones: (1) two early Pleistocene to late Pliocene volcanoes, (2) five mid-Pleistocene volcanoes, and (3) two youngest late Pleistocene to Holocene volcanoes. The two earliest volcanoes are Xishan volcano (2.8 Ma, whole-rock K—Ar age, Liu et al., 1990) and Matishan volcano (1.63 Ma whole-rock K-Ar age, Liu et al., 1990). These two volcano cones have been partially eroded. The five mid-Pleistocene volcanoes include Daheishan volcano (also named No. 2 (Zhao, 1976)), Yishan volcano (No. 4 volcano), Migongshan volcano, Yueyashan volcano, and Maoniushan volcano. Their $^{40}Ar/^{39}Ar$ eruption ages derived from sanidine cluster around 270 ka.

The two youngest volcanoes in the AVF are Ashishan volcano and Wulukeshan volcano. The compositions of their volcanic products range from 52 wt% SiO_2 to 57 wt% SiO_2 (Cooper et al., 2002). Ashishan volcano, also known as "No. 1" volcano (Zhao, 1976), is located to the south of the Ashikule Lake (Fig. 1b) and is a well-preserved truncated conical edifice. A lava flow field from Ashishan covers an area of 33 km^2. Most Ashishan lavas erupted at 66 ka based on $^{40}Ar/^{39}Ar$ dating of sanidines (Dunbar et al., 1996). The youngest eruption was reported to occur on May 27, 1951 (Liu et al., 1990), but it is unclear if this eruption produced lava flows. Wulukeshan volcano, also known as "No. 3" volcano (Zhao, 1976), is situated near the northeastern corner of Wuluke Lake (Fig. 1b), and is also a well-preserved truncated conical edifice. Wulukeshan has produced widespread lava flows. In the southwestern direction, Wulukeshan lavas flowed into the Wuluke Lake. Due to their young ages, these two volcanoes are ideal for studying high-resolution timescales of magmatism below thick (>60 km) continental crust in a continental collision zone.

3. Methods

Zircons were separated using standard density and magnetic methods from 3 samples (513-09, 513-07, 513-4b) from Ashishan volcano and 1 sample (WLK2) from Wulukeshan volcano. Samples 513-09 (35°41′55″N, 81°34′40″E) and 513-07 (35°41′56″N, 81°34′46″E) were collected near the rim of Ashishan volcano, and sample 513-4b (35°42′39″N, 81°36′15″E) was collected 3 km northeast of the Ashishan volcanic cone (Fig. 1c). Individual zircon grains were hand-picked and embedded into soft indium metal to analyze unpolished zircon rim U-Th isotope compositions. Zircons are enriched in U relative to Th with significant amounts of initial $^{238}U/^{230}Th$ disequilibrium, allowing for the dating of the pre-eruption history of a magma up to 375 ka (Reid et al., 1997). With sampling depths of only about 3 μm, secondary ion mass spectrometry (SIMS) depth profiling of unpolished zircon crystals embedded into indium allows crystallization ages to be derived from U—Pb (Reid and Coath, 2000) or U-Th disequilibrium (Schmitt et al., 2010; Zou et al., 2010a) geochronology with higher spatial resolution than conventional spot analyses of sectioned crystals.

^{238}U-^{230}Th compositions of zircon crystals were analyzed by SIMS using the Stanford-U.S. Geological Survey (USGS) SHRIMP-RG ion microprobe (for samples 513-07, 513-4b and part of 513-09) and the UCLA CAMECA ion microprobe 1270 (for part of 513-09 and WLK2). Analytical methods at Stanford-USGS SHRIMP-RG lab for ^{238}U-^{230}Th depth profiling have been documented in Vazquez and Lidzbarski (2012) and Marcaida et al. (2019). Analytical methods at UCLA for ^{238}U-^{230}Th depth profiling have been documented in Zou et al., 2010a and Schmitt (2011). Secondary electron images of selected zircons reflecting zircon flat tomography are given in Appendix.

4. Results

4.1. Ashishan volcano

Twenty-five zircon grains from 513-09 were analyzed for U-Th isotopes. Seven grains plot on the equiline with equal ($^{230}Th/^{232}Th$) and ($^{238}U/^{232}Th$) values and a slope of unity, indicating secular equilibrium and crystallization ages >375 ka. Eighteen grains show ^{238}U-^{230}Th disequilibrium (Fig. 2) and yield an isochron age of 100 ± 33 ka (2σ) using Isoplot (Ludwig, 2003), but with a high MSWD (mean squared weighted deviates) of 5.2 and probability of fit of zero, indicative of more than one age population. Unmixing of zircon model age data into Gaussian populations (Sambridge and Compston, 1994) yields two populations; a majority population (65%) at 70.3 ± 6.3 ka (2σ,) and a minority (35%) at 105 ± 15 ka (Fig. 3). These 2 age populations do not overlap within their uncertainties, consistent with more than one age population. Zircon grains older than 375 ka have U contents of 132–3940 ppm, Th contents of 123–778 ppm, and Th/U ratios of 0.20–1.47 (Supp Table 1). Zircon grains younger than 375 ka have U contents of 76–1260 ppm, Th contents of 132–543 ppm, and Th/U ratios of 0.35–1.84 (Table 1).

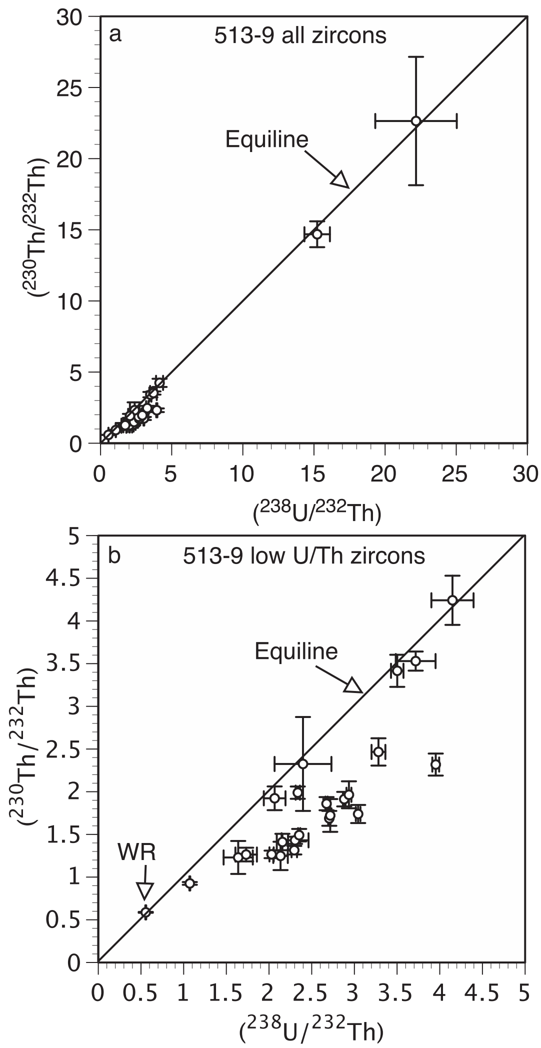

Fig. 2. Zircon U-Th isotope diagram for 513-09 from Ashishan. Fig. 2a includes 2 high U/Th zircons in ^{238}U-^{230}Th secular equilibrium whereas Fig. 2b excludes these two high U/Th zircons for clarity. The whole-rock data is from Cooper et al. (2002). WR = whole rock. Equiline defines secular equilibrium and indicates ages older than 375 ka.

Sixteen zircon grains from 513-07 were also analyzed. Thirteen grains plot on the equiline and the other 3 grains show ^{238}U-^{230}Th disequilibrium with model ages of ~75 ka, 90 ka, 170 ka (Fig. 5). The 75-ka model age is similar to the 70-ka population from 513-09 and the model ages of 90 ka and 170 ka are similar to the 105-ka population from 513-09 within error. Among the 13 zircons on the equiline, two zircon grains display very high (>300) U/Th activity ratios (Fig. 4). If we combine the 18 young grains from 513-09 with the 3 young grains from 513-07, unmixing of their model ages yield two pulses at 71.9 ± 5.6 and 106 ± 16 ka, which are similar to the peaks of 70 ka and 105 ka obtained from 513-09 alone. Zircons grains older than 375 ka have U contents of 53–3110 ppm, Th contents of 4–698 ppm, and Th/U ratios of 0.004–1.19 (Supp Table 1). Zircons grains younger than 375 ka have U contents of 340–648 ppm, Th contents of 155–303 ppm, and Th/U ratios of 0.37–0.77 (Table 1).

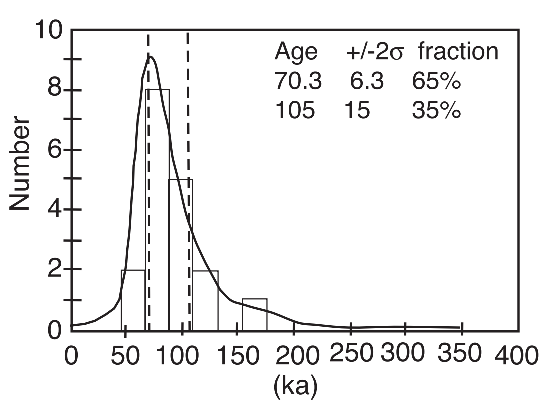

Fig. 3. Unmixing ages for zircons from 513-09 using the algorithm by Sambridge and Compston (1994).

Thirteen zircon grains from 513-4b, a different lava flow than 513-09 and 513-07 from Ashishan (Fig. 1c), were analyzed for U-Th isotopes. Eleven grains plot on the equiline, suggesting ages >375 ka. Two zircon grains yield model ages of ~295 ka and ~285 ka (Fig. 5). These two zircon grains and the whole rock composition yield a 291 ± 77 ka isochron date, which is similar to the ~270 ka pulse of volcanism indicated by ^{40}Ar/^{39}Ar dating of sanidine. Zircon grains older than 375 ka have U contents of 91–1782 ppm, Th contents of 12–695 ppm, and Th/U ratios of 0.07–0.74 (Supp Table 1). Zircon grains younger than 375 ka have U contents of 512–539 ppm, Th contents of 163–284 ppm, and Th/U ratios of 0.32–0.53 (Table 1).

4.2. Wulukeshan volcano

Five zircons from WLK2 were analyzed for U-Th isotopes. Four grains plot on the equiline (Fig. 6), indicating crystallization ages of >375 ka. Two zircon grains plot below the equiline and have zircon-melt model ages of ~100 ka and 125 ka. The isochron date from these two zircon grains and their whole rock composition is 113 ± 34 ka (Fig. 6). Their model ages and isochron age are similar to the 105-ka population from 513-09. Zircons older than 375 ka have U contents of 445–2120 ppm, Th contents of 229–954 ppm, and Th/U ratios of 0.30–0.76 (Supp Table 1). Zircons younger than 375 ka have U contents of 660–1858 ppm, Th contents of 268–355 ppm, and Th/U ratios of 0.19–0.41 (Table 1).

Old (>375 ka) zircons plotting on the equiline are present in all 4 samples, in proportions of 28% (n = 7/25) for 513-09, 81% (n = 13/16) for 513-07, 85% (n = 11/13) for 513-4b, and 67% (n = 4/6) for WLK2. Abundant (~60%) old zircons demand for dating of individual crystal grains, as the complexities cannot be resolved by bulk analysis methods.

5. Discussions

5.1. Young volcanism in NW Tibet at high temporal resolution

Our high-resolution U-Th zircon age data can be used to compare with earlier K-Ar and Ar-Ar ages to provide constraints on the timing of volcanism at high temporal resolution.

5.1.1. Ashishan volcano

Dating of Ashishan volcanic products indicate mid- to late-Pleistocene magmatism. Liu et al. (1990) reported a whole-rock K-Ar age of 120 ± 20 ka for an Ashishan lava flow, and Xu et al. (2014) reported 3 whole-rock ^{40}Ar/^{39}Ar ages of 80 ± 60 ka, 170 ± 10 ka, and 460 ± 40 ka. ^{40}Ar/^{39}Ar analyses of sanidine crystals yielded a pulse at ~66 ka for Ashishan (Dunbar et al., 1996). Thermoluminescence dating of sandstone xenoliths in the Ashishan lavas indicated an eruption age of 74 ± 4 ka (Deng, 1991).

Because zircon rim crystallization must predate a volcanic eruption, U-Th zircon ages should be older than K-Ar or Ar-Ar eruption ages, although they may overlap within their uncertainties. Zircon saturation temperatures (Boehnke et al., 2013) for the Ashishan magmas are ~700–750 °C, although this saturation model is not specifically derived for alkaline compositions. Eruption temperatures are undetermined, but the presence of euhedral zircons suggests that the host magmas

Table 1
U-Th isotope and concentration data for Ashikule young zircon rims measured by depth profiling.

Sample	(^{238}U/^{232}Th)	1 s	(^{230}Th/^{232}Th)	1 s	Th age ka	1S.E. + ka	1S.E. - ka	U ppm	Th ppm	Th/U
Ashi-shan										
513-9-1.1	2.157	0.066	1.411	0.096	78.8	15.3	13.4	129	183	1.41
513-9-2.1	2.337	0.025	1.989	0.072	168.9	23.9	19.6	164	213	1.30
513-9-3.1	2.305	0.158	1.431	0.042	71.8	11.0	10.0	313	418	1.34
513-9-4.1	2.135	0.085	1.248	0.166	59.2	22.4	18.5	376	543	1.44
513-9-9.1	1.639	0.171	1.230	0.193	98.2	74.6	43.9	76	140	1.84
513-9-11.1	2.296	0.032	1.315	0.050	59.1	5.8	5.5	192	253	1.32
513-9-13.1	2.030	0.025	1.266	0.044	67.3	6.5	6.2	197	295	1.50
513-9-15.1	3.044	0.027	1.739	0.106	67.8	9.1	8.4	233	232	0.99
513-9_1	2.706	0.013	1.688	0.087	78.4	9.6	8.8	192	171	0.89
513-9_2	2.353	0.013	1.491	0.073	76.4	9.5	8.7	219	169	0.77
513-9_3	2.881	0.015	1.913	0.085	92.3	9.9	9.0	254	240	0.95
513-9_4	2.717	0.015	1.722	0.192	81.4	22.7	18.8	180	161	0.89
513-9_5	3.953	0.040	2.318	0.129	77.8	8.9	8.3	192	249	1.30
513-9_6	1.072	0.005	0.926	0.016	116.7	13.4	11.9	1263	445	0.35
513-9_10	2.674	0.013	1.860	0.077	100.3	10.6	9.7	451	396	0.88
513-9_11	3.282	0.081	2.466	0.160	127.6	24.4	19.9	157	170	1.08
513-9_12	2.936	0.029	1.964	0.158	94.4	18.8	16.1	136	132	0.96
513-9_14	1.732	0.126	1.264	0.080	93.6	26.8	21.5	466	265	0.57
513-7-4.1	3.904	0.203	2.452	0.169	88.8	16.1	14.0	395	303	0.77
513-7-11.1	6.703	0.176	3.650	0.136	75.2	5.9	5.6	340	155	0.46
513-7-15.1	8.152	0.485	6.558	0.474	168.1	51.1	34.7	648	240	0.37
513-4b_1.1	5.763	0.175	5.409	0.211	284	128	57	539	284	0.527
513-4b_11.1	9.546	0.162	8.971	0.206	294	59.9	39	512	163	0.319
Wuluke										
WLK2_4	15.867	0.563	9.632	1.441	97.6	29.4	23.1	1858	355	0.19
WLK2_6	7.475	0.207	5.260	0.450	122.9	25.7	20.8	660	268	0.41

Whole-rock (^{238}U/^{232}Th) = 0.556±0.005 and (^{230}Th/^{232}Th) = 0.587±0.005 from Cooper et al. (2002) are used for age calculation.
S.E. = standard error.
Old (>375 ka) zircons with U-Th secular equilibrium are provided in supplemental Table A.1.

were zircon saturated. Most of the whole-rock ^{40}Ar/^{39}Ar and K-Ar dates (e.g., 120 ka, 170 ka, 460 ka) are older than the zircon age peak at ~70 ka. These older dates from whole-rock samples may be biased toward older ages if, as is suggested by the presence many old (>375 ka) zircons, there is a cargo of antecrystic major phases. Although the 80 ± 60 ka whole-rock ^{40}Ar/^{39}Ar age is close to 70 ka, this age has a large error. The apparent peak of crystallization at 70 ka for zircons from samples 513-09 and 513-07 is similar to the ~66 ka eruption age from ^{40}Ar/^{39}Ar sanidine dating (Dunbar et al., 1996) as well as the thermoluminescence age at 74 ± 4 ka (Deng, 1991). In addition, it is noteworthy that the 105-ka population from 513-09 is similar to a sanidine ^{40}Ar/^{39}Ar date of 100 ± 3 (1σ) ka from Ashishan (Cooper et al., 2002), suggesting recycling of zircons from this earlier episode of magmatism and volcanism.

Sample 513-4b has only one peak at ~291 ka and lacks younger populations at 70 ka and 105 ka, suggesting that this lava flow erupted earlier than 513-09 and 513-07. We note that a pulse of trachyandesitic activity occurred at around 270 ka, based on ^{40}Ar/^{39}Ar dating of sanidine phenocrysts from several other volcanic centers from AVF (Dunbar et al., 1996). Our U-Th zircon work suggests that this 270-ka pulse also occurred at Ashishan.

5.1.2. Wulukeshan volcano

Whole-rock K-Ar dating of a Wulukeshan lava yielded a date of 200 ± 50 ka (Liu et al., 1990), while whole-rock ^{40}Ar/^{39}Ar dating yielded dates of 290 ± 60 Ma, 540 ± 50 Ma, and 550 ± 60 ka (Xu et al., 2014). All these whole-rock ages are older than the ~115-ka zircon crystallization age from this study. Because any zircon growth precedes volcanic eruptions and zircon retains U and Th because of their slow diffusion in zircon even at magmatic temperature, zircon U-Th crystallization ages provide a maximum limit on eruption age. We propose that the eruption of the Wulukeshan lavas occurred after or about the same time as the ~115 ka peak in crystallization. As the Wulukeshan rocks contain many old crystals, whole-rock K-Ar or Ar-Ar ages can be biased toward older ages. A better constraint on the Wulukeshan eruption age is likely to be provided by ^{40}Ar/^{39}Ar dating of single sanidine crystals.

5.2. Zircon and magma residence time scales

Despite experimental studies suggesting unfavorable conditions for zircon crystallization, zircons have been found to form early in potassic magmas (Bergman, 1987; Bucholz et al., 2017). Accordingly, zircon residence times can be used to date magma storage times (e.g., Bucholz et al., 2017). If we use the apparent young peak of zircon crystallization at 70 ± 3 ka (Fig. 3) and eruption age of 66 ± 1 ka for the youngest Ashishan pulse, then the zircon residence time would be around 4 ± 3 ka. The 105-ka zircon population (Fig. 3) should come from magmas older than the 70-ka population but younger than 105 ka. Of the 6 ^{40}Ar/^{39}Ar ages in Cooper et al. (2002), AKB-10 (122 ka) is too old, and AKB-2, AKB-4, AKB-5, and AKB-6 have similar eruption ages around 70 ka. Thus, only sample AKB-1 (100 ± 3 ka) has the sensible eruption age. Therefore, the apparent zircon residence time for the 105 ± 8 ka zircon population is 5 ± 8 ka. This inference should be tested in the future by measuring ages of zircons directly from 100-ka samples. With regard to the 291-ka zircon crystallization, when compared to the reported eruptive episode at 270 ka, a zircon residence time of ~21 ± 77 ka is suggested. Owing to the large uncertainty (77 ka) for the 21-ka residence time for older zircons, we select zircon residence times with small errors and suggest that zircon residence time is short (<5 kyr) for these post-collisional potassic magmas even though the magmas passed through thick continental crust in northern Tibet. Based on the presence of ^{230}Th/^{238}U excesses in Ashishan lavas, Cooper et al. (2002) concluded that any magma residence was no more than tens of kyr. Short magma residence time scales are not common for andesitic and felsic magmas in arc settings (e.g., Garrison et al., 2012; Simon et al., 2008), but have been reported for some continental volcanoes at Mount Changbai (Zou et al., 2010b; Zou et al., 2014) and Acigol (Schmitt et al., 2011). Wulukshan lacks a precise and accurate

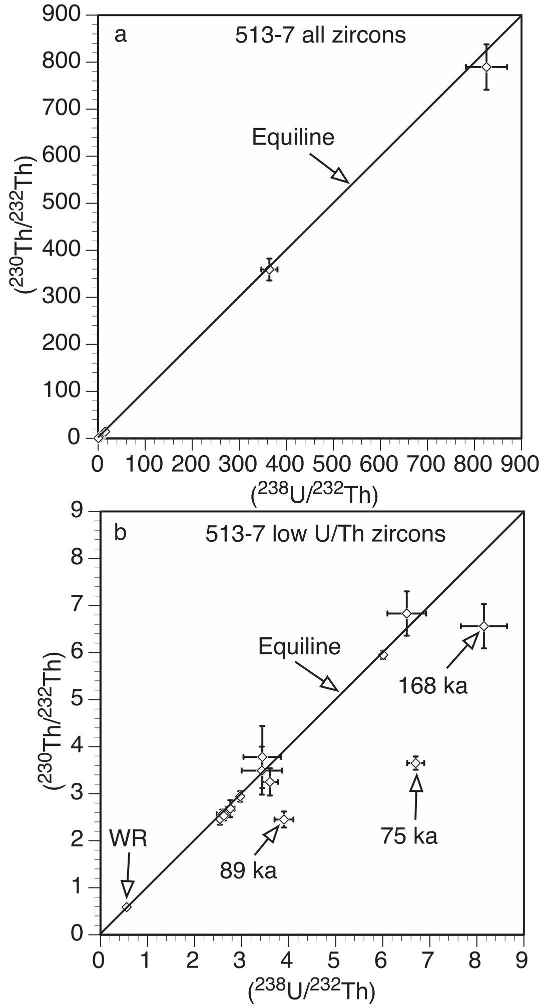

Fig. 4. Zircon U-Th isotope diagram for 513-07 from Ashishan. Fig. 4a includes two very high U/Th zircons in ^{238}U-^{230}Th secular equilibrium whereas Fig. 5b excludes these two very high U/Th zircons. WR = whole rock. Equiline defines secular equilibrium and indicate ages older than 375 ka.

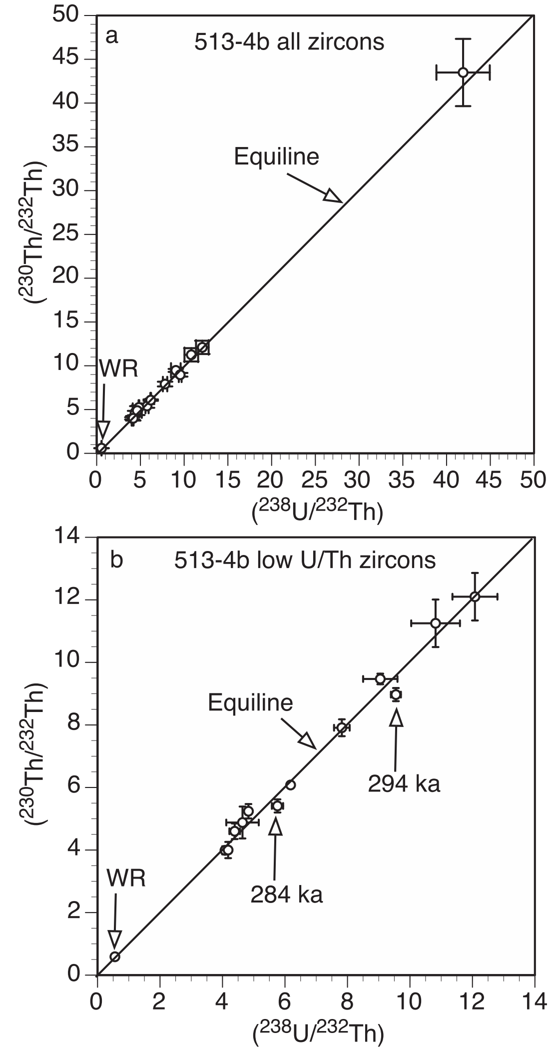

Fig. 5. Zircon U-Th isotope diagram for 513-4b from Ashishan. Fig. 5a includes one high U/Th zircon in ^{238}U-^{230}Th secular equilibrium whereas Fig. 5b excludes this high U/Th zircon. WR = whole rock. Equiline defines secular equilibrium and indicate ages older than 375 ka.

eruption age, which prevents an estimation of zircon residence time for its magma.

5.3. Relation between Ashishan and Wulukeshan at 105 ka

Wulukeshan is thought to have formed during an earlier episode than Ashishan because of its older whole-rock K-Ar and Ar-Ar ages. Our study reveals that Wulukeshan contains zircons that crystallized at ~113 ka, which is younger than previously reported K-Ar or Ar-Ar ages. Thus, the eruption age for Wulukeshan is <113 ka, similar to the eruption age of ~100 ka for Ashishan. Similarities in their zircon age spectra suggests that zircon crystallization occurred at Ashishan and Wulukeshan during to the same eruption episode. In addition, the similar zircon crystallization ages of ~105–113 ka indicate that the Ashishan and Wulukeshan magmatic systems were active at the same time. Since Ashishan and Wulukeshan are rather close (15 km) and their zircon ages are similar at ~105 ka, the magma systems responsible for Ashishan and Wulukeshan may have tapped the same subvolcanic magmatic reservoir at 105 ka and these eruptions, but that would require a caldera-scale reservoir. Similar major element compositions between WLK2 (SiO_2 = 56.33%, TiO_2 = 1.84%) and the Ashikule samples (e.g., 513-07 with SiO_2 of 55.86% and TiO_2 of 1.86%) are consistent with this interpretation.

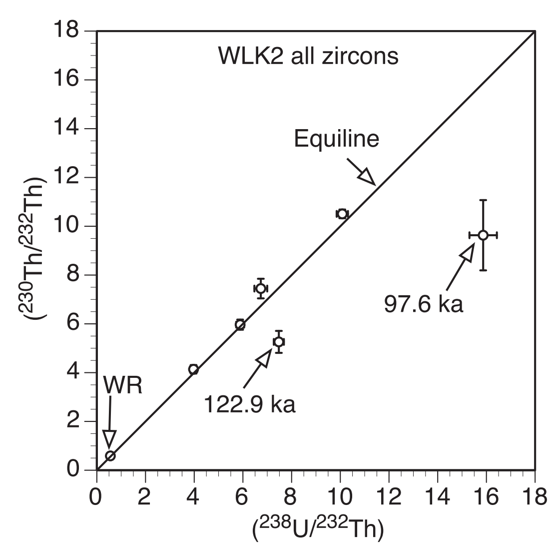

Fig. 6. Zircon U-Th isotope diagram for WLK2 from Wulukeshan. WR = whole rock.

5.4. Implications for the generation and evolution of potassic magmas beneath NW Tibet

Subjective implications of this study from petrological perspectives are several. First, the origin of the potassic magma must have involved phlogopite melting, that is stable to a depth of 200 km (Enggist et al., 2012). This phlogopite might have formed by a subduction zone hybridization process (Wyllie and Sekine, 1982), a tectonic setting akin to the current NW Tibetan volcanic field. Our study indicate that magma transport is fast for these deep potassic magmas formed in this type of tectonic setting. Another implication of the short residence time of zircon in effusive magma chambers, like this study, may be of significance for the high precision zircon U/Pb dating of the lava formations in the Deccan (Schoene et al., 2019) that were supposed to be derived from distal effusive acidic magma chambers synchronously (Basu et al., 2018). The short zircon residence time established in this paper strengthens the argument of Basu et al. (2018).

6. Conclusions

(1) We have identified 3 pulses of zircon crystallization at 70 ka, 105 ka, and 290 ka for the Ashishan volcano and one pulse of zircon crystallization at 113 ka for the Wulukeshan volcano.
(2) Similarity between zircon U-Th ages and eruption ages for the Ashishan volcano suggests short zircon and magma residence times (<5 kyr) for post-collisional potassic volcanism beneath thick continental crust.
(3) An eruption around 270 ka likely to have occurred at Ashishan.
(4) New zircon U-Th age of 113 ka for Wulukeshan requires that the Wulukeshan eruption occurred after 113 ka, younger than previously thought. Old crystals likely contributed to their older whole-rock K-Ar or Ar-Ar ages.
(5) Similar zircon peak at 105–113 ka for Ashishan and Wulukeshan likely indicates an interconnected subsurface magma reservoir for these two young volcanoes during their eruption.
(6) The high abundance of geologically old (>375 Ka) zircons demand for crystal-scale (in addition to whole-rock scale) isotope studies for the widespread post-collisional lavas in continental collision zones.

Acknowledgements

We thank Axel Schmitt, Mae Marcaida, and Marty Grove for their assistance with ion probe analyses at UCLA and Stanford-USGS SHRIMP-RG. We are grateful to Asish Basu and Jifeng Xu for journal reviews, to Mark Stelten and Mike Clynne for USGS internal reviews, and to Mike Roden for editorial handling and reviews. These reviews have significantly improved the quality of this paper. This work was in part supported by National Natural Science Foundation of China [NSFC grant number 41272070]. Any use of trade, firm, or product names is for descriptive purposes only and does not imply endorsement by the U.S. Government.

Declaration of Competing Interests

The authors declare that they have no known competing financial interests or personal relationships that could have appeared to influence the work reported in this paper.

Appendix A. Supplementary data

Supplementary data to this article can be found online at https://doi.org/10.1016/j.lithos.2020.105418.

References

Basu, A.R., Chakrabarty, P., Ibamez-Mejia, M., Georg, R.B., Ghosh, N., 2018. U-Pb zircon ages of Deccan acid igneous complexes and their temporal relationship with the Cretaceous-Paleogene boundary. Goldschmidt Abstracts 145.
Bergman, S.C., 1987. In: Fitton, J.G., Upton, B.G.J. (Eds.), Lamproites and other potassium-rich igneous rocks: A review of their occurrence, mineralogy and geochemistry. Geological Society of London Special Publication, Alkaline Igneous Rocks, pp. 103–190.
Boehnke, P., Watson, E.B., Trail, D., Harrison, T.M., Schmitt, A.K., 2013. Zircon saturation re-revisited. Chem. Geol. 351, 324–334.
Bucholz, C.E., Eddy, M.P., Jagoutz, O., Bowring, S.A., Schmidt, M.W., Sambuu, O., 2017. Constraining the time scales of magmatic differentiation with U-Pb zircon geochronology. Geology 45, 11–14.
Chen, J.L., Xu, J.F., Wang, B.D., Kang, Z.Q., 2012. Cenozoic Mg-rich potassic rocks in the Tibetan Plateau: Geochemical variations, heterogeneity of subcontinental lithospheric mantle and tectonic implications. J. Asian Earth Sci. 53, 115–130.
Chen, J.L., Wu, J.B., Xu, J.F., Dong, Y.H., Wang, B.D., Kang, Z.Q., 2013. Geochemistry of Eocene high-Mg# adakitic rocks in the northern Qiangtang terrane, Central Tibet: Implications for early uplift of the plateau. Geol. Soc. Am. Bull. 125, 1800–1919.
Chung, S., Chun, M., Zhang, Y., Xie, Y., Lo, C., Lee, T., Lan, C., Li, X., Zhang, Q., Wang, Y., 2005. Tibetan tectonic evolution inferred from spatial and temporal variations in post-collisional magmatism. Earth Sci. Rev. 68, 24.
Cooper, K.M., Reid, M.R., Dunbar, N.W., McIntosh, W.C., 2002. Origin of mafic magmas beneath northwestern Tibet: Constraints from ^{230}Th-^{238}U disequilibria. Geochem. Geophys. Geosyst. https://doi.org/10.1029/2002GC000332.
Deng, W.M., 1978. A preliminary study on the petrology and petrochemistry of the Quaternary volcanic rocks of northern Tibet autonomous region. Acta Geol. Sin. 52, 148–162.
Deng, W.M., 1991. Geology, geochemistry and age of shoshonitic lavas in the central Kunlun orogenic belt. Acta Geol. Sin. 201–213.
Ding, L., Kapp, P., Zhong, D., Deng, W., 2003a. Cenozoic volcanism in Tibet: evidence for a transition from oceanic to continental subduction. J. Petrol. 44, 33.
Ding, L., Kapp, P., Zhong, D.L., Deng, W.M., 2003b. Cenozoic volcanism in Tibet: evidence from oceanic to continental subduction. J. Petrol. 44, 1833–1865.
Dunbar, N.W., Phillips, F.M., McIntosh, W.C., 1996. Uplift of the Northern Tibetan Plateau: Insights from ^{40}Ar/^{39}Ar and Cl-36 analysis of young lava flows. Eos. Trans. AGU T21B–18.
Enggist, A., Chu, L.L., Luth, R.W., 2012. Phase relations of phlogopite with magnesite from 4 to 8 GPa. Contrib. Mineral. Petrol. 163, 467–481.
Flower, M.F., Tamaki, K., Hoang, N., 1998. Mantle extrusion: A model for dispersed volcanism and DUPAL-like asthenosphere in East Asia and the West Pacific. In: Flower, M.F.J., Chung, S.L., Lo, C.H., Lee, T.Y. (Eds.), Mantle Dynamics and Plate Interaction in East Asia. Am. Geophys. Union, Washington, D. C, pp. 67–88.
Gao, Y.G., Hou, Z.Q., Kamber, B.S., Wei, R.H., Meng, X.J., Zhao, R.S., 2007. Lamproitic rocks from a continental collision zone: evidence for recycling of subducted Tethyan oceanic sediments in the mantle beneath southern Tibet. J. Petrol. 48, 729–752.
Garrison, J.M., Reagan, M.K., Sims, K.W.W., 2012. Dacite formation at Ilopango Caldera, El Salvador: U-series disequilibrium and implications for petrogenetic processes and magma storage time. Geochem. Geophys. Geosyst. 13, Q06018.
Guo, Z.F., Wilson, M., Liu, J.Q., Mao, Q., 2006. Post-collisional, potassic and ultrapotassic magmatism of the northern Tibetan Plateau: Constraints on characteristics of the mantle source, geodynamic setting and uplift mechanisms. J. Petrol. 47, 1177–1220.
Liu, D., Zhao, Z.D., Zhu, D.C., Niu, Y.L., DePaolo, D.J., Harrion, T.M., Mo, X.X., Dong, G.C., Zhou, S., Sun, C.G., Zhang, Z.C., Liu, J.L., 2014. Postcollisional potassic and ultrapotassic rocks in southern Tibet: Mantle and crustal origins in response to India-Asia collision and convergence. Geochim. Cosmochim. Acta 143, 207–231.
Liu, F., Li, X., Wang, G.Q., Liu, Y.F., Zhu, H.L., Kang, J.T., Huang, F., Sun, W.D., Xia, X.P., Zhang, Z.F., 2017. Marine Carbonate Component in the Mantle Beneath the Southeastern Tibetan Plateau: evidence from Magnesium and Calcium Isotopes. J. Geophys. Res. Solid Earth 122, 9729–9744.
Liu, J.Q., Maimaiti, Y.M., Yi, M., 1990. K-Ar ages and distribution of volcanoes in western Kunlun. Science in China 180–187.
Ludwig, K.R., 2003. User's Manual for ISOPLOT 3.00: a geochronological toolkit for Microsoft Excel, Berkeley.
Marcaida, M., Vazquez, J.A., Stelten, M.E., Miller, J.S., 2019. Constraining the early eruptive history of the Mono Craters Rhyolites, California, based on ^{238}U-^{230}Th isochron dating of their explosive and effusive products. Geochem. Geophys. Geosyst. 20, 1539–1556.
Miller, C., Schuster, R., Klotzli, U., Frank, W., Purtscheller, F., 1999. Post-collisional potassic and ultrapotassic magmatism in SW Tibet: Geochemical and Sr-Nd-Pb-O isotopic constraints for mantle source characteristics and petrogenesis. J. Petrol. 40, 1399–1424.
Mo, X.X., Hou, Z.Q., Niu, Y.L., Dong, G.C., Qu, X.M., Zhao, Z.D., Yang, Z.M., 2007. Mantle contributions to crustal thickening during continental collision: evidence from Cenozoic igneous rocks in southern Tibet. Lithos 96, 225–242.
Reid, M.R., Coath, C.D., 2000. In situ U-Pb ages of zircons from the Bishop Tuff: no evidence for long crystal residence times. Geology 28, 443–446.
Reid, M.R., Coath, C.D., Harrison, T.M., McKeegan, K.D., 1997. Prolonged residence times for the youngest rhyolites associated with Long Valley caldera: Ion microprobe dating of young zircons. Earth Planet. Sci. Lett. 150, 27–38.
Sambridge, M.S., Compston, W., 1994. Mixture modeling of multi-component data sets with application to ion-probe zircon ages. Earth Planet. Sci. Lett. 128, 18.
Schmitt, A.K., 2011. Uranium series accessory crystal dating of magmatic processes. Annu. Rev. Earth Planet. Sci. 39, 321–349.

Schmitt, A.K., Wetzel, F., Cooper, K.M., Zou, H.B., Worner, G., 2010. Magmatic longevity of Laacher See Volcano (Eifel, Germany) indicated by U-Th dating of intrusive carbonatites. J. Petrol. 51, 1053–1085.

Schmitt, A.K., Danišík, M., Evans, N.J., Siebel, W., Kiemele, E., Aydin, F., Harvey, J.C., 2011. Acigöl rhyolite field, Central Anatolia (part 1): high-resolution dating of eruption episodes and zircon growth rates. Contrib. Mineral. Petrol. 162, 1215–1231.

Schoene, B., Eddy, M.P., Samperton, K.M., Keller, C.B., Keller, G., Adatte, T., Khadri, S.F., 2019. U-Pb constraints on pulsed eruption of the Deccan Traps across the end-Cretaceous mass extinction. Science 363, 862–866.

Shen, H.H., Xu, J.D., Yu, H.M., Zhao, B., Ji, L.Y., 2014. Study on the volcanic edifice and petrological, mineralogical caracteristics of Ashi Volcano in west Kunlun Mountains. Seismology and Geology 36, 105–122.

Simon, J.I., Renne, P.R., Mundil, R., 2008. Implications of pre-eruptive magmatic histories of zircons for U-Pb geochronology of silicic extrusions. Earth Planet. Sci. Lett. 266, 182–194.

Turner, S.P., Hawkesworth, C., Liu, J., Rogers, N., Kelley, S., Van Calsteren, P., 1993. Timing of Tibetan uplift constrained by analysis of volcanic rocks. Nature 364, 50–53.

Turner, S.P., Arnaud, N., Liu, J., Rodgers, N., Hawkesworth, C., Harris, N., Kelley, S., Van Calsteren, P., Deng, W., 1996. Post-collision, shoshonitic volcanism on the Tibetan Plateau: Implications for convective thinning of the Lithosphere and the Source of ocean island basalts. J. Petrol. 37, 45–71.

Vazquez, J.A., Lidzbarski, M.I., 2012. High-resolution tephrochronology of the Wilson Creek Formation (Mono Lake, California) and Laschamp event using 238U-230Th SIMS dating of accessory mineral rims. Earth Planet. Sci. Lett. 357–358, 54–67.

Wang, Q., Wyman, D.A., Xu, J.F., Dong, Y.H., Vasconcelos, P.M., Pearson, N., Wan, Y.S., Dong, H., Li, C.F., Yu, Y.S., Zhu, T.X., Feng, X.T., Zhang, Q.Y., Zi, F., Chu, Z.Y., 2008. Eocene melting of subducting continental crust and early uplifting of Central Tibet: evidence from central-western Qiangtang high-K calc-alkaline andesites, dacites and rhyolites. Earth Planet. Sci. Lett. 272, 158–171.

Williams, H.M., Turner, S.P., Peace, J.A., Kelley, S.P., Harris, N.B.W., 2004. Nature of the source regions for post-collisional, potassic magmatism in southern and northern Tibet from geochemical variations and inverse trace element modelling. J. Petrol. 45, 555–607.

Wyllie, P.J., Sekine, T., 1982. The formation of mantle phlogopite in subduction zone hybridization. Contrib. Mineral. Petrol. 79, 375–380.

Xia, L.Q., Li, X.M., Ma, Z.P., Xu, X.Y., Xia, Z.C., 2011. Cenozoic volcanism and tectonic evolution of the Tibetan plateau. Gondwana Res. 19, 850–866.

Xu, J.D., Zhao, B., Sindney, H., Chen, Z.Q., Zhang, L.Y., 2014. Geological features and eruption history of Ashikule volcano clusters in western Kunlun Mountain. Acta Petrol. Sin. 30, 3521–3530.

Zhao, M.Y., 1976. Introduction of Ashikule active volcanoes and the Quaternary volcano groups in Kunlun Mountains of Xinjiang. Xinjiang Geol. 1-2, 27–36.

Zhao, Z., Mo, X., Dilek, Y., Niu, Y., DePaolo, D.J., Robinson, P., Zhu, D., Sun, C., Dong, G., Zhou, S., Luo, Z., Hou, Z., 2009. Geochemical and Sr–Nd–Pb–O isotopic compositions of the post-collisional ultrapotassic magmatism in SW Tibet: Petrogenesis and implications for India intra-continental subduction beneath southern Tibet. Lithos 113, 190–212.

Zou, H.B., Fan, Q.C., Schmitt, A.K., Sui, J.L., 2010a. U-Th dating of zircons from Holocene potassic andesites (Maanshan volcano, Tengchong, SE Tibetan Plateau) by depth profiling: Time scales and nature of magma storage. Lithos 118, 202–210.

Zou, H.B., Fan, Q.C., Zhang, H.F., 2010b. Rapid development of the great Millennium eruption of Changbaishan (Tianchi) Volcano: evidence from U-Th zircon dating. Lithos 119, 289–296.

Zou, H.B., Fan, Q.C., Zhang, H.F., Schmitt, A.K., 2014. U-series zircon age constraints on the plumbing system and magma residence times of the Changbai volcano, China/North Korea border. Lithos 200-201, 169–180.